Journal of Groundwater Science and Engineering
ISSN 2305-7068
Indexed by ESCI CABI CSA Scopus GeoRef AJ CNKI

Investigation of groundwater characteristics and its influence on Landslides in Heifangtai Plateau using comprehensive geophysical methods

Feng-dan Yu, Gang Qiao, Kai Wang, Xu Zhang

Citation:
Yu FD, Qiao G, Wang K, *et al*. 2023. Investigation of groundwater characteristics and its influence on Landslides in Heifangtai Plateau using comprehensive geophysical methods. Journal of Groundwater Science and Engineering, 11(2): 171-182.

View online: https://doi.org/10.26599/JGSE.2023.9280015

Journal homepage: http://gwse.iheg.org.cn

Research Paper

Investigation of groundwater characteristics and its influence on Landslides in Heifangtai Plateau using comprehensive geophysical methods

Feng-dan Yu[1,2], Gang Qiao[1,2*], Kai Wang[1], Xu Zhang[1,2]

[1] *Key Laboratory for Groundwater and Ecology in Arid and Semi-arid Areas*, *Xi'an* 710054, *China*.
[2] *Xi'an Center of Geological Survey*, *China Geological Survey*, *Xi'an* 710054, *China*.

Abstract: The occurrence of landslides in Heifangtai plateau is primarily caused by the rise in water levels due to irrigation. To accurately understand the distribution of groundwater and its impact on the landslide hazard, a combination of Electrical Resistivity Tomography (ERT), Induced Polarization (IP) and Surface Nuclear Magnetic Resonance (SNMR) methods were used in this study. By conducting a comprehensive analysis, the characteristics of water-bearing structure in vertical and groundwater distribution in horizontal were detected; and the influence of the groundwater on plateau and landslides was also identified. The results indicate that the groundwater occurs in the loess aquifer with a three-layer structure in vertical. Horizontally, the aquifer has a unified water table over the plateau, with a low water level in the north and high one in the south. The high resistivity bedrock uplift belt in the middle of the plateau forms a watershed, with the north side of the uplift belt being a relatively stable slope area with stable water content and fewer geological disasters. In contrast, the south side of the uplift belt is a disaster-prone region with vertical fissures well developed in the loess aquifers. The southern landslides are characterized by the interphase distribution of high and low electrical resistivity. The infiltration and discharge of groundwater result in the formation of a collapse belt in the low resistivity water-bearing structure of landslide, which causes the entire block with high resistivity and stable bedrock to slide. There was a newly formed landslide in a larger range at the landslide's trailing edge. This study provides a scientific basis for the study of landslides mechanisms and disaster prevention by identifying the distribution characteristics of groundwater and analyzing its influence from a geophysical perspective in Heifangtai.

Keywords: ERT; IP; SNMR; Distribution characteristics; Uplift belt; Sliding surface

Received: 14 Jul 2022/ Accepted: 11 Apr 2023/ Published: 15 Jun 2023

Introduction

Disasters such as landslides and loess collapse caused by water diversion and irrigation in Heifangtai are serious problem that has been extensively researched (Cao et al. 2016; Hou et al. 2018; Lian et al. 2020). The high frequency of landslides in the region has garnered attention from scholars worldwide and is often referred to "modern landslide natural laboratory" (Derbyshire et al. 1994; Derbyshire, 2001; Xu et al. 2008; Xu et al. 2019).

Extensive research has shown that the softening of abutting rocks and soil due to groundwater infiltration caused by extensive agricultural irrigation is the primary factor leading to landslides in Heifangtai (Wang and Liu, 1999; Wang and Hui, 2001; Wang et al. 2004; Zhu, 2019; Zhou et al. 2020; Ye et al. 2021). To understand the groundwater infiltration mechanism and loess landslide initiation mechanism in Heifangtai, scholars have conducted in-depth studies, elaborating on lands-

*Corresponding author: Gang Qiao, *E-mail address*: qgcyboy@163.com

DOI: 10.26599/JGSE.2023.9280015

Yu FD, Qiao G, Wang K, et al. 2023. Investigation of groundwater characteristics and its influence on Landslides in Heifangtai Plateau using comprehensive geophysical methods. Journal of Groundwater Science and Engineering, 11(2): 171-182.

lide type, development characteristics and other related topics (Jin and Dai, 2007; Wu et al. 2011; Xu et al. 2009; Wu et al. 2019; Zhao et al. 2017; Zhang et al. 2022). Based on these findings, experts have developed several methods for monitoring and early warning of landslides, successfully predicting their timing (Xu et al. 2016; Zhang et al. 2017). Geophysicists have also contributed to this field, using techniques such as electrical resistivity tomography (ERT) to detect local groundwater (Zhang et al. 2017), electrical tomography to analyze the relationship between resistivity and water content (Bian et al. 2020), and geological radar and ERT to describe preferential flow passage such as small loess cracks (Tian et al. 2019).

Previous studies have largely focused on the mechanism and prediction of landslides in Heifangtai, with limited drilling data for the analysis of groundwater in the plateau, and geophysical work limited to small areas near landslides zones. However, a comprehensive understanding of the large-scale distribution and variation of groundwater in Heifangtai as well as the influence of groundwater runoff and discharge on plateau and landslides, remain elusive.

To address this knowledge gap, a combination of electrical resistivity tomography (ERT), induced polarization (IP) and surface nuclear magnetic resonance (SNMR) was employed, based on geological data and published literature. ERT is an array type of electrical detection system based on electrical differences in electrical conductivity (Song et al. 2020; Cesar et al. 2021), while the method of IP uses electrical differences in rock strata to identify aquifers (Achref et al. 2017; Rustadi et al. 2022). SNMR is the only geophysical method that can directly detect water (Lu et al. 2021). The integration of these three methods can overcome the limitations and ambiguities of a single geophysical prospecting method and provide more reliable results (Yu et al. 2014). The resistivity information obtained from ERT and IP can be used to interpret the SNMR inversion interpretation and identification of aquifer posions, while ERT and IP can identify false electromagnetic interference anomalies for SNMR. Although SNMR has limited detection depth and is less effective in areas with large electromagnetic interference, the water-bearing trend from the depths can be detected by IP and ERT, and the combination of the three methods can more accurately identify the location of aquifers.

1 Study area

Fig. 1 shows the location of Heifangtai, located near Yanguoxia City, Yongjing County, Gansu Province, at the junction of the Yellow River and the Huangshui River. This region is a part of the Hekou-Minhe Basinwhich belongs to the eastern segment of the Laji-Wusu fold belt in the Qilian orogenic belt.

Fig. 2 shows Heifangtai loess plateau that is nearly isolated from the nearby topography. The northern edge of plateau is Moshigou, with a depth of 30–110 m and a valley slope of 13°–40°. The southern edge of the plateau is connected to the II Terrace of Yellow River, with a height difference of 60–131 m and a slope of 20°–50°. The steep and elevated terrain surrounding the plateau creates favorable conditions for landslides.

The geological structure of Heifangtai exhibits great complexity. The plateau's stratification consists of Upper Pleistocene aeolian loess at the top, followed by Middle Pleistocene alluvial silty clay, and finally the Lower Cretaceous estuary group composed of sandy gravel and sandy mudstone (Song et al. 2018; Zeng and Jia, 2022). Groundwater in Heifangtai is mainly distributed in the pores of loess and gravel, as well as the fissures in bedrock.

In the past, Heifangtai experienced an arid climate with limited precipitation and high evaporation rate, resulting in a scarcity of groundwater in its natural state. The loess aquifer system lacked a continuous distribution of the regional unified phreatic surface, and there were few landslides around the plateau. However, since 1968, flood irrigation has been used for agricultural purposes, causing the groundwater level of the loess aquifer to steadily rise above its top surface due to the barrier of relatively water-resistant silty clay layer. By 1980, the groundwater level had risen by 9 m and by 2012, the increase was close to 20 m, with an average increase of 0.27 m/a. Particularly since 2005, large-scale promotion of vegetal greenhouses and orchards has increased irrigation, further driving the rise of groundwater level, and leading to a subsequent increase in the frequency of landslides. According to statistics, the number of landslides has gradually increased since the beginning of agricultural irrigation in 1968, indicating its significant impact on the landslides in Heifangtai (Dong et al. 2013; Jia et al. 2013).

Landslides in Heifangtai can be classified into two genetic type: Loess bedrock landslides and loess internal landslides (Zhao et al. 2016). Bedrock landslides are mainly developed on the south and west sides of the plateau, characteristized by large volume and multiple slides. On the other

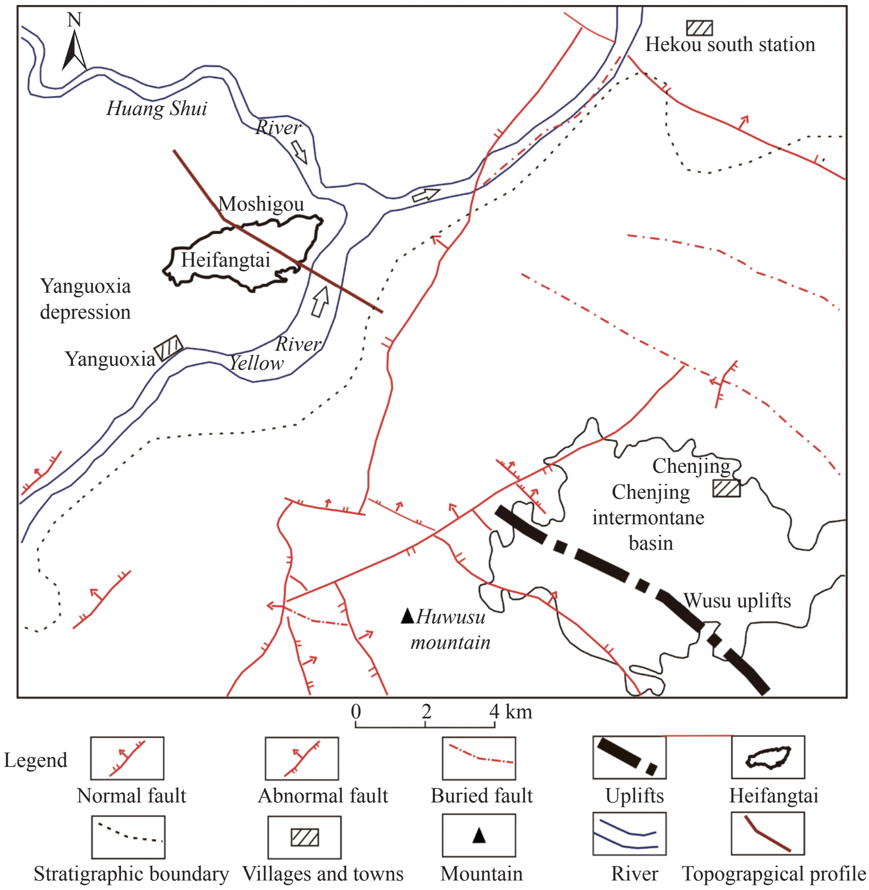

Fig. 1 Structural diagram of Heifangtai area①

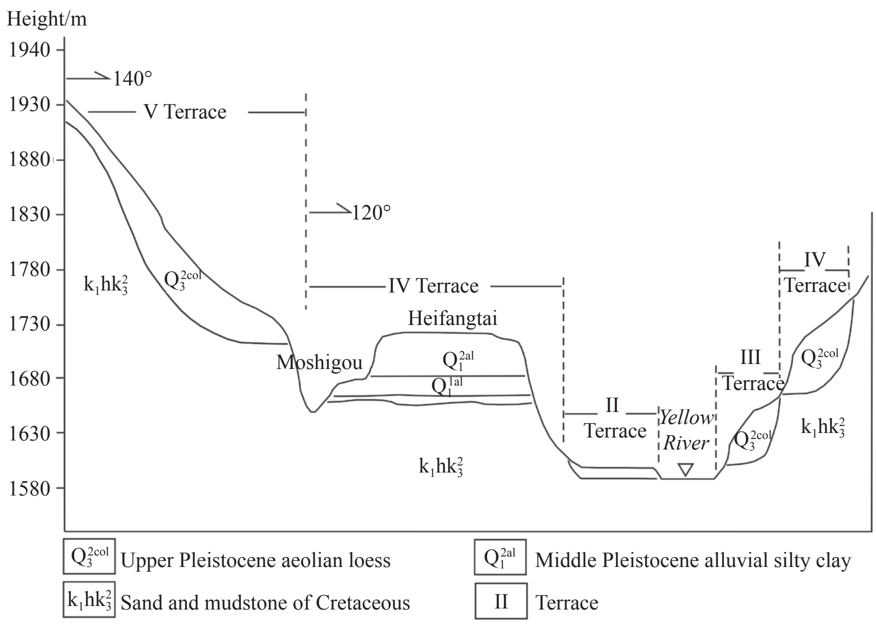

Fig. 2 Topographical profile across Heifangtai (Wang et al. 2017)

hand, loess internal landslides are mainly developed on the east side of the plateau, characterized by high sliding speeds and strong destructive forces. The continuous rise of groundwater level in the loess layer in recent years has led to an increase in the frequency of loess landslides in Heifangtai.

① Xi'an CGS. Investigation Report on Loess Landslide in Heifangtai Area of Gansu Province. 2016.

2 Methods

2.1 Selection of study methods

Table 1 demonstrates the result of original minerals in loess gradually that migrate downward and lead to high resistivity in the upper part and low resistivity in the lower part of aquifer, caused by the infiltration of irrigation water. This phenomenon provides a basis for the use of I electrical prospecting techniques, such as ERT and IP, in the region.

Prior to conducting formal work, instrument validity testing was performed to ensure adequate measurement parameters and high-quality raw data. Based on experimental comparison, the Wenner device was selected for ERT, while the symmetrical quadrupole device positioned 5 m from the power supply pole was chosen for IP. To minimize interference, the SNMR coil was designed in an 8-square shape. The technical parameters of each method are provided in Table 2.

Table 1 Logging formation resistivity in Heifangtai

Lithology	Status	Resistivity range /Ohm·m
Loess	Dry aqueous	100–200 5–80
Silty clay		10–300
Sand and gravel		5–100
Sandstone-mudstone		3–50

2.2 Work deployment

As shown in Fig. 3, three ERT measurement profiles were deployed along the plateau in the western, central and eastern parts, covering a total length of 6 800 m. The primary objective of the ERT was to explore the electrical structure characteristics of the plateau and slope. Additionally, six SNMR points were located in close proximity to the II-1 ERT profile due to the presence of hillside villages and challenging terrain. These points were mainly used to determine the position of aquifer, permeability and water content. Six IP points were

Table 2 Technical parameters

Working method	Technical parameters	
SNMR	Coil: 8-character square; Superimposition times: 128; Pulse distance: 40 ms.	Side length: 75 m; Number of pulse distance: 16;
IP	Device: Symmetric quadrupole; Supply electrode distance: 5 m	Maximum supply electrode distance: 400 m;
ERT	Device: Wenner; Electrode spacing: 5–10 m.	Maximum section length: 2 900 m;

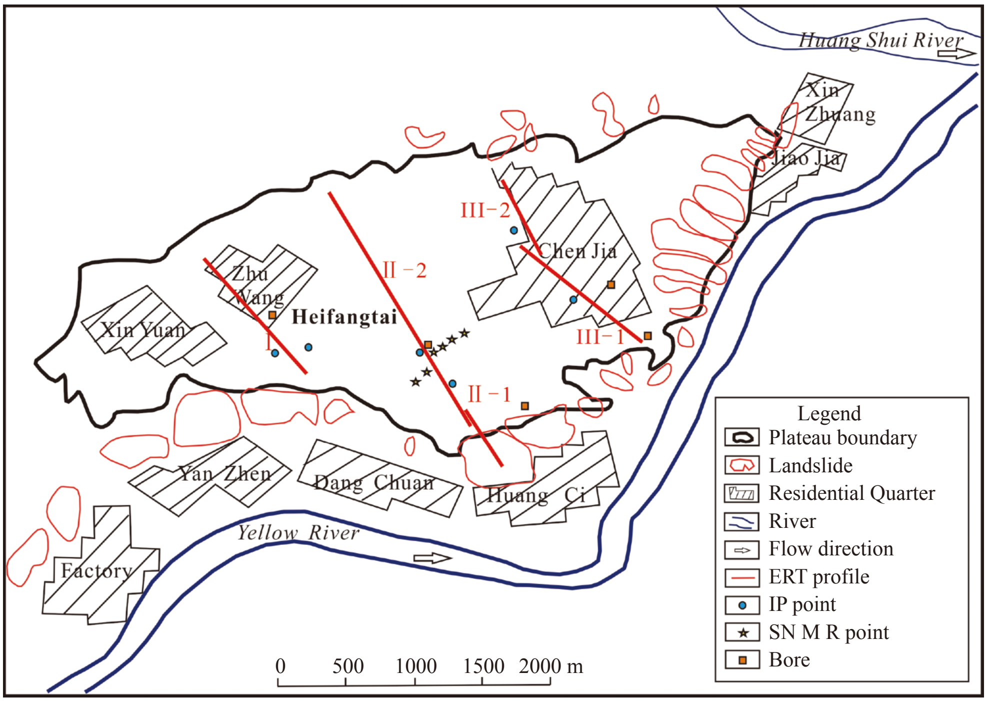

Fig. 3 Layout of geophysical survey

evenly distributed near the ERT profiles, in order to provide valuable information for joint interpretation with the other two methods.

2.3 Data processing

Due to the presence of undulating terrain, poor ground conditions and position displacement, the measured values in practice may not be consistent with the theoretical model. Therefore, it is necessary to pre-process the raw data through techniques such as data splicing, terrain correction and elimination of false points. In processing the data from the ERT profiles, the Res2Dinv software was used for inversion calculation and graph design. After 3 to 4 iterations, the fit error was less than 8%, and the inversion results were closer to the real situation. SNMR was processed using the NUMIS software, and eight inversion layers are selected, based on the electrical characteristics of the strata. The IP was plotted directly using the observed resistivity values.

3 Results and discussion

3.1 Water-bearing structure

Based on Fig. 4, the SNMR results intuitively show that the groundwater in the plateau can be divided into three layers from top to bottom.

The water content and location of the shallow loess aquifer are highly unstable due to climatic factors and local irrigation conditions, as evidenced by low water content and permeability at SNMR points H3, H4, H5, H6 the permeability is low.

The porous and fissured loess aquifer has low porosity and permeability, and the depth and thickness of the aquifer vary significantly, making it the primary cause of loess landslides at the edge of the plateau. Due to the presence of vertical joints, large pores and swallowing holes, vertical permeability of the loess is much higher than the horizontal one (Ren et al. 2020). It is believed that precipitation is mostly absorbed by the thick loess layer, with only a small portion infiltrating to the bottom of the loess layer through fast channels such as vertical cracks and swallow holes, forming the porous and fissured loess aquifer above the silty clay layer.

The sandy gravel and bedrock aquifer, with a high water content and good permeability, is the main aquifer in this area. The sandy gravel layer is located under the silty clay layer in the bedrock of the Cretaceous Hekou Group and above the IV Terrace of the Yellow River. Drilled hole data reveal that a thickness of 5 m to 7 m and particle size ranging from 2 mm to 10 mm, and with a dense state in the sandy gravel layer. Although the silty clay layer is impermeable, the groundwater at the bottom of the loess layer can slowly infiltrate through pores or skylights of the silty clay layer and then discharges deep along the weathered bedrock fracture belt, forming the sandy gravel and bedrock aquifer.

Table 3 presents data from experimental tests and SNMR inversion on bedrock aquifer location

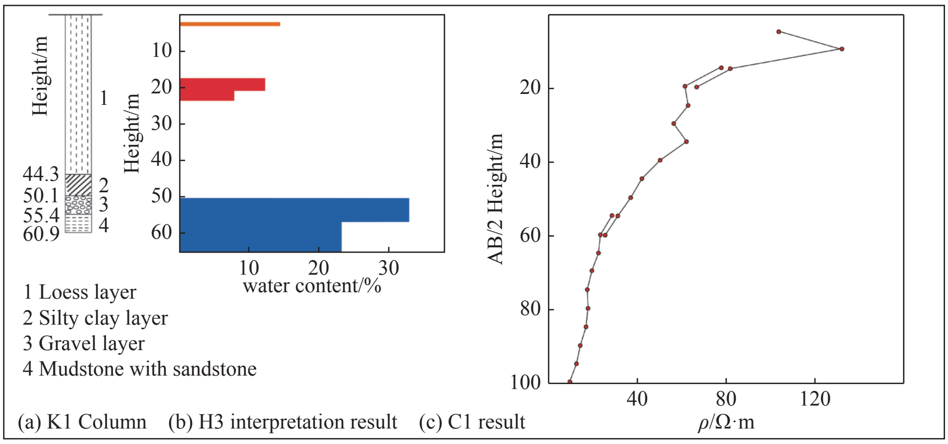

Fig. 4 Results of logged column of bore K1, SNMR H3 and IP C1

Table 3 Technical parameters

Experimental tests		SNMR inversion		Discrepancy rate /%
Static water level depth (m)	51.32	Upper interface of bedrock aquifer (m)	50.43	1.73
Bedrock water Content (%)	25.73	Bedrock water Content (%)	23.65	8.17

and water content. The discrepancy rate for the bedrock aquifer location is 1.73%, and the bedrock water content, it is 8.17%. The two results are in agreement, indicating the reliability and accuracy of the SNMR data.

3.2 Plateau disaster scope division

The ERT profiles provide resistivity data at different depths, which are used to generate planar isolines to illustrate the electrical trend surface. Based on the ERT profiles and drilling data, it is estimated that the buried depth of bedrock is approximately 50–60 m in Heifangtai. The 50 m and 65 m depth resistivity planar isoline are used to infer the fluctuation of water-bearing bedrock surface based on the electrical parameters.

Fig. 5 shows the 50 m deep resistivity planar isoline, which indicates that the high resistivity region is located in the south and west of the plateau, with resistivity values ranging from about 8 Ohm·m to 14 Ohm·m. Along the northeast direction, the resistivity value gradually decreases, and the resistivity gradient changes uniformly, reflecting the consistent changes in water content, salt content and soil structure in the Quaternary loess layer.

Fig. 6 is the 65 m deep resistivity planar isoline, which shows that the high resistivity region in the west and south is expanded, with resistivity values ranging from 8 Ohm·m to 12 Ohm·m. The low resistivity region is mainly concentrated in the northern part of the plateau, with resistivity values ranging from about 3 Ohm·m to 6 Ohm·m, and the area of low resistivity is further reduced. It is hypothesized that there is a relatively high resistivity anomaly belt in the center of the plateau, which is disconnected in the middle. Combining with the drilling data, it is inferred to be a bedrock uplift belt.

As shown in Fig.7, the rise of groundwater level has led to the formation of a unified phreatic interface in the region, with the low water levels occur in the north and high in the south. The II-2 profile can be divided into two sections based on the electrical difference. The low resistivity values of 1 800–2 900 m appear in a large region, indicating that the aquifer is saturated. However, it is interesting to note that that there is also farmland irrigation in the northern part of the Heifangtai, despite the presence of fewer springs and less landslides occurred on the slope. This can be attributed to factors such as the influence of topogra-

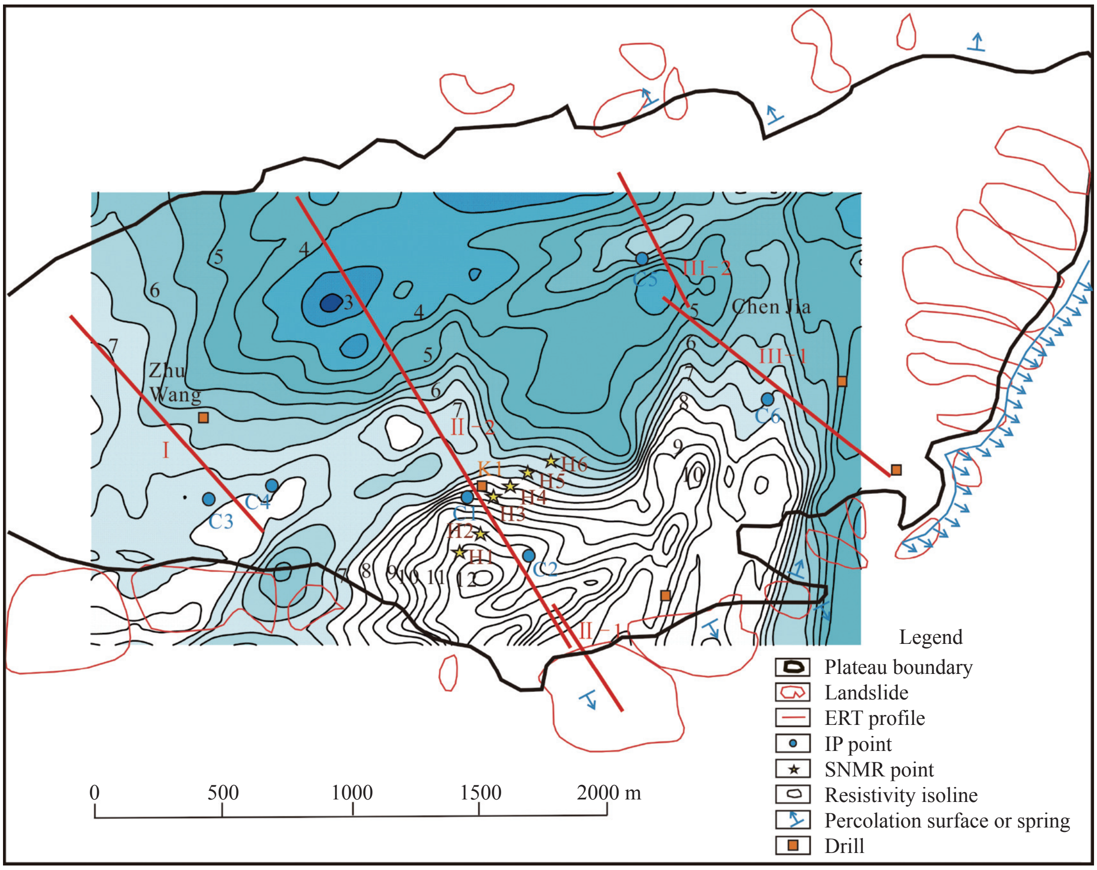

Fig. 5 Resistivity planar isoline of 50 m depth

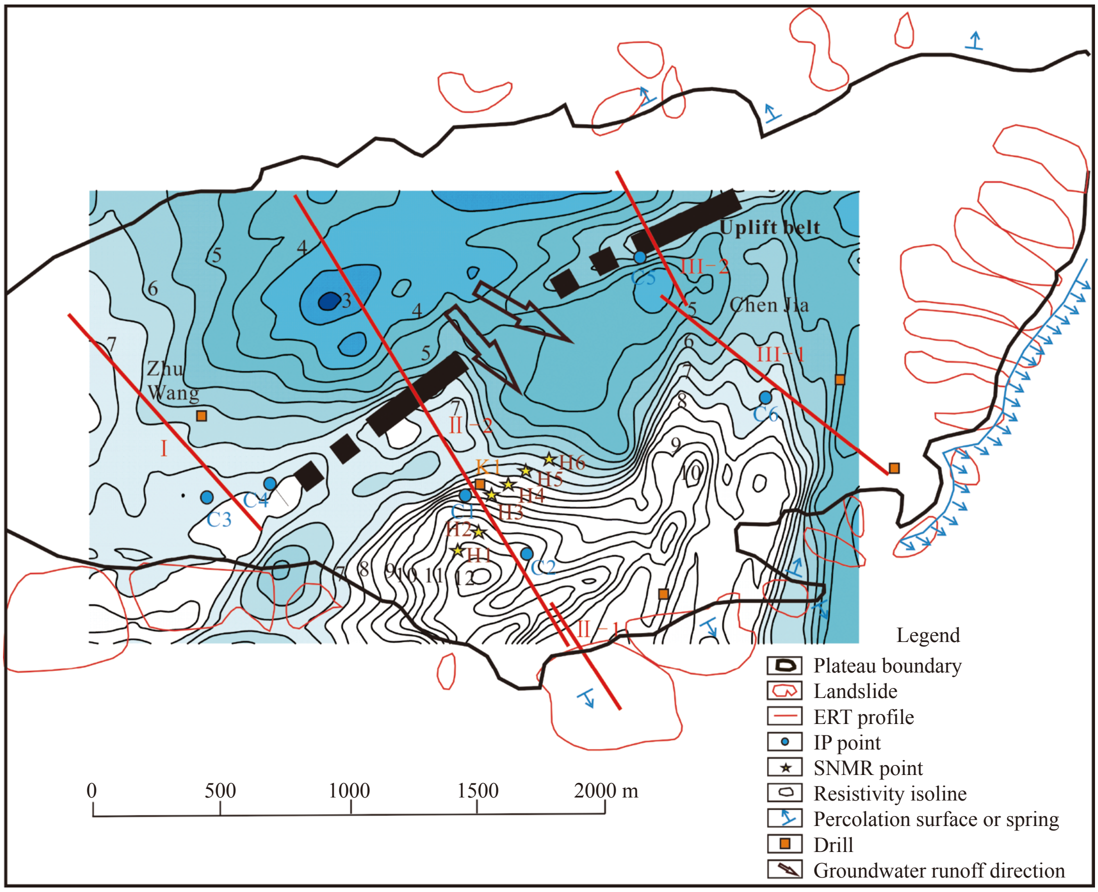

Fig. 6 Resistivity planar isoline of 65 m depth

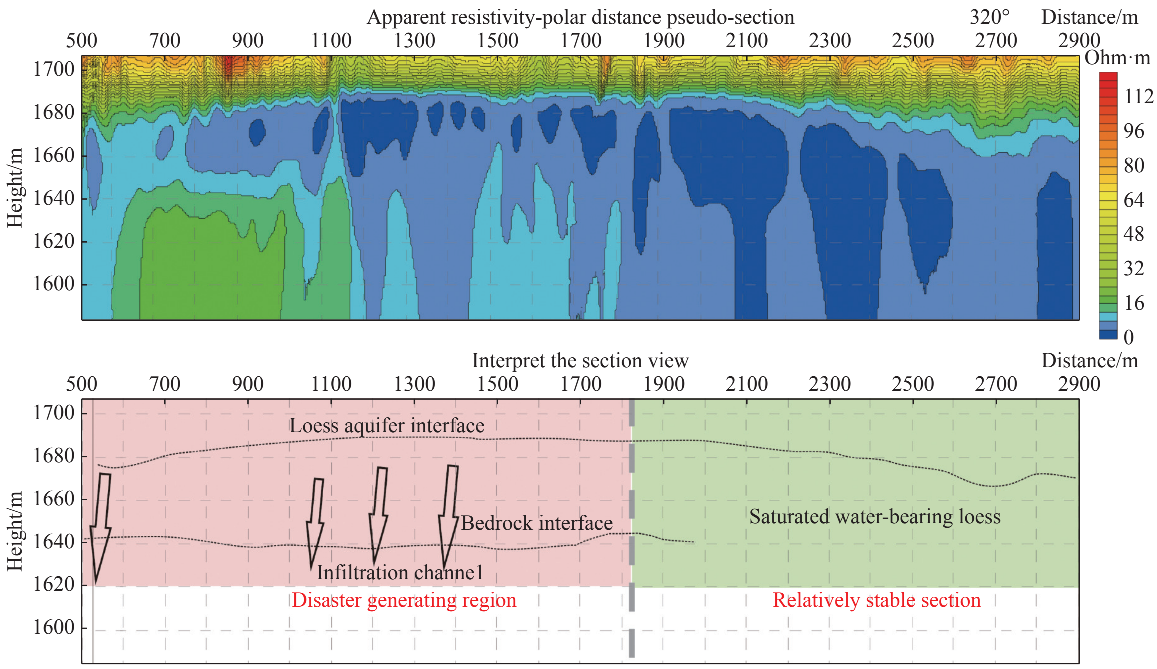

Fig. 7 Ⅱ-2 ERT profile interpretation

phy, change in water-resisting layer elevation, and others, which cause the groundwater to flow southeastward. As the middle of the bedrock uplift belt is discontinuous, after the infiltration of irrigation water, most of the groundwater flows southeastward along the low surface relief section between the bedrock uplift belt, resulting in slower groundwater level rise and smaller impact on the slope. Therefore, the water-bearing state of the strata in the section of 1 800–2 900 m is considered to be relatively stable at present. On the other hand, the resistivity value of 500–1 800 m is higher and unevenly distributed than the north side, indicating a high resistivity of vertical shear. This distribution is close to the edge of the plateau on the south side, and the vertical characteristics of the formation resistivity are evident, suggesting that vertical drainage cracks in the loess layer have developed. As a result, the groundwater flows rapidly along the cracks, with surface expressions as seepages or springs, leading to the development of landslides. Therefore, the water-bearing strata in this section are considered to be unstable.

Based on Fig. 8, it can be inferred that the bedrock uplift creates a natural division between two regions. The groundwater state on the north side of the uplift belt is currently stable, indicating a relatively stable region. In contrast, groundwater on the south side can rapidly recharge through farmland irrigation, together with groundwater flows from the north, leading to complete desalination of the loess and triggering the loess landslides, making it a disaster-prone area.

It should be noted that in the stable region on the north side of the uplift belt, continuous irrigation may lead to a rise in groundwater level, which eventually change the existing groundwater equilibrium field. This will increase the impact of groundwater on the northern slope, gradually intensifying the landslides in the region.

3.3 The influence of groundwater on landslides

Fig. 9 illustrates three zones of low resistivity on the slope of profile II-1. The centers of low resistivity anomalies are located at approximately 100 m, 180 m and 260 m in the section, respectively. The low resistivity regions at the top and bottom of the slope are large and not confined, with resistivity values ranging from 2 Ohm·m to 12 Ohm·m. The low resistivity region in the middle of the slope is small, approximately 40 m in width, and dips southward. In this zone, the resistivity values range from 2 Ohm·m to 10 Ohm·m. Two high resistivity zones are situated between the low resistivity sections: The lower one is about 40 m wide, with an abnormal resistivity value ranging from 35 Ohm·m to 95 Ohm·m, and the upper one is about 25 m wide, with an

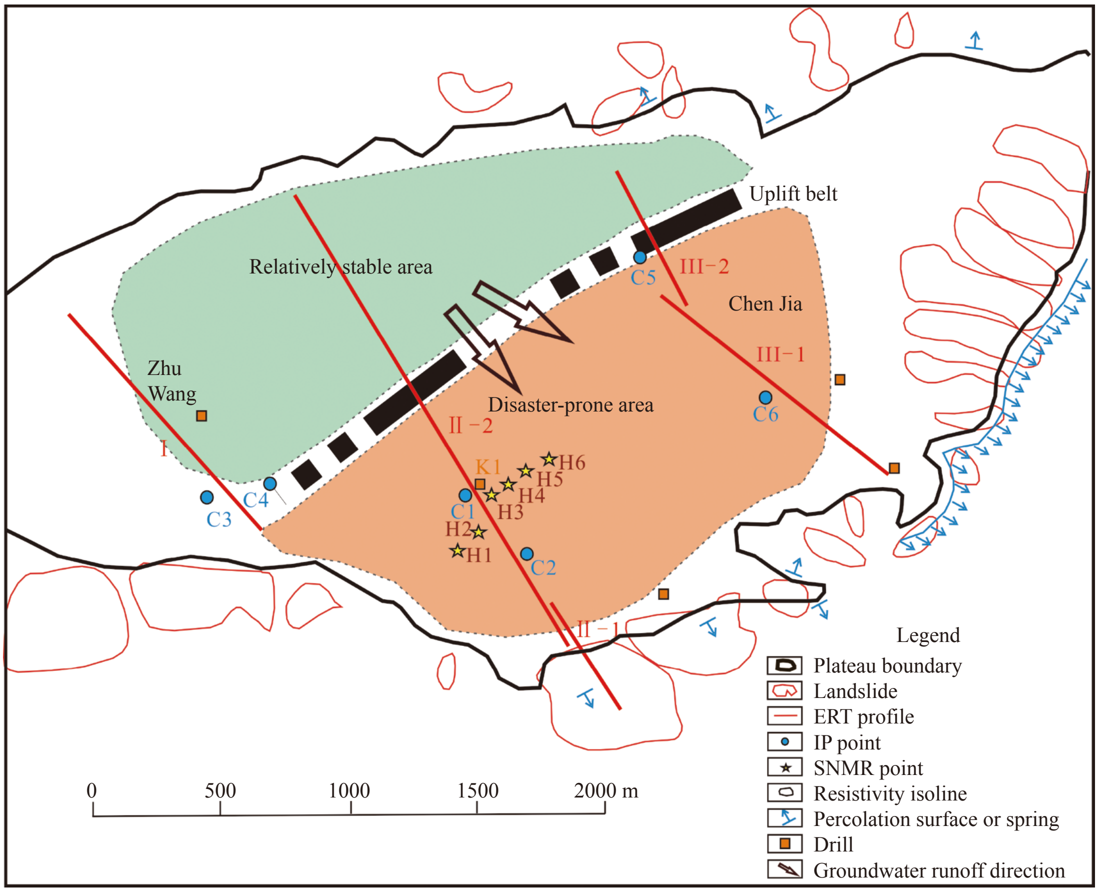

Fig. 8 Disasters affected zoning diagram

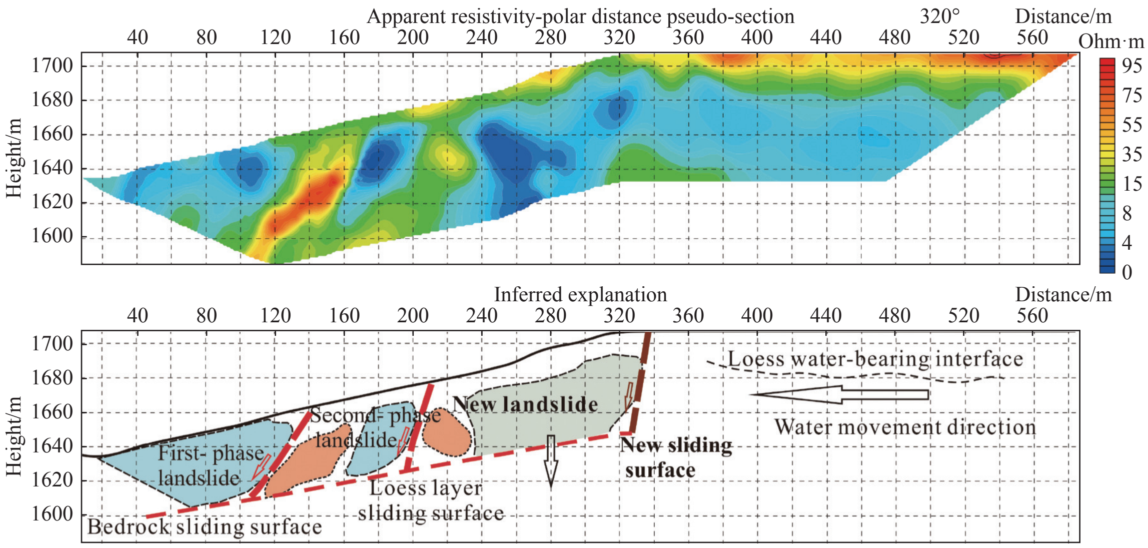

Fig. 9 Ⅱ-1 ERT profile interpretation

abnormal resistivity value ranging from 20 Ohm·m to 40 Ohm·m.

In the loess-bedrock area, several landslides have occurred in recent years, with sliding surfaces traversing the layer between loess at the upper and bedrock at the bottom. ERT results suggest that the landslide has two phases of landslide characteristics on the slope. The first-phase landslide is located near 120 m, with a slide body that exhibits low resistivity characteristics due to high water content. Seeping groundwater is exposed as springs in front of the landslide. The second-phase landslide is located near 200 m, with a sliding body composed of both low and high resistivity zones. A saturated layer is forms at the bottom of the loess layer due to the continuous infiltration of groundwater, which reduces the resistance of the loess. After the formation of a small collapse, the new free surface has a discharging effect on the backwall of the landslide, and the sliding surface is formed at the interface between low and high resistivity. The slope with high resistivity is relatively stable due to its low water content, and it may slide in the form of entire sliding block.

High and low resistivity zones bands at the landslide' s trailing edge are wider, with the low resistivity zone almost perpendicular to the edge of the plateau. This suggests that irrigation water discharges downward along the dominant channels in the loess layer, which further expands the original holes and fissures. Once the discharge channel is formed, it becomes an inherited dominant infiltration channel (Xu et al. 2017). Because of strong mechanical erosion, the upper part of the slope will collapse, forming a new sliding surface. Therefore, it is considered that a new landslide is formed. Water may continue to infiltrate to the bedrock, which smooths the bedding plane and reduces slope stability, resulting in the formation of the bedrock sliding surface in the weak structural plane at the sand-mud intercalated layers.

4 Conclusion

The study reveals that the groundwater in the plateau is characterized as a three-layer structure at depth. Groundwater in the shallow loess is unevenly distributed. The porous and fissured loess aquifer has low porosity and permeability, which is the main layer responsible for geological disasters. Besides, the gravel and bedrock layers have a high water content and good permeability, making them the main aquifer in the region.

Furthermore, the study finds that a unified phreatic interface has formed in the previously localized loess aquifer in the region. The loess aquifer interface exhibits low characteristics in the north and high characteristics in the south, with a relatively high resistivity uplift in the middle of the plateau. It is inferred that the north of the uplift belt is relatively stable, while vertical fractures of the water-bearing loess layer are well developed in the south of the uplift belt, leading to the formation of sliding beds and inducing numerous loess landslides, indicating that it is a disaster-prone area.

This study analyzes the sliding characteristics of landslides under the influence of groundwater flow and discharge from a geophysical perspective. The infiltration and convergence of groundwater forms a collapse belt in the low resistivity body of the landslide, causing the entire block to slide out of the upper high resistivity stable region. Moreover, the study identifies a newly formed landslide of greater amplitude on the trailing edge of the landslide, which requires further investigation.

Acknowledgement

This study was supported and funded by the National Natural Science Foundation of China (Grant No: 42177346, 52009103), the Key Laboratory for Groundwater and Ecology in Arid and Semi-arid Areas, and the China Geological Survey project (No: DD20190296). We are grateful to the anonymous reviewers for their valuable suggestions in improving the manuscript.

References

Achref C, Belgacem R, Hakim G, et al. 2017. Combined application of vertical electrical sounding and 2D electrical resistivity imaging for geothermal groundwater characterization: Hammam Sayala hot spring case study (NW Tunisia). Journal of African Earth Sciences, 134(10): 292−298. DOI：10.1016/j.jafrearsci.2017.07.003.

Bian SQ, Yang YP, Ma JH, et al. 2020. Two-dimensional imaging study of internal moisture in loess slope: A case study of the Luojiapo landslide in Heifangtai terrace. Journal of Engineering Geology, 28(4): 840−851. (in Chinese) DOI：10.13544/j.cnki.Jeg.2019-345.

Cao CW, Xu Q, Peng DL, et al. 2016. Research on the failure mechanism of the Heifangtai loess landslides based on the physical simulation experiments. Hydrogeology & Engineering Geology, 43(4): 72−77. (in Chinese) DOI：10.16030/j.cnki.issn.1000-3665.2016.04.12.

Cesar AM, Vania R, Lucas MF, et al. 2021. Hydraulic conductivity and geophysics (ERT) to assess the aquifer recharge capacity of an inland wetland in the Brazilian Savanna. Environmental Challenges, 12(5): 1−10. DOI：10.1016/j.envc.2021.100274.

Derbyshire E, Dijkstra TA, Smalley IJ, et al. 1994. Failure mechanisms in loess and the effects of moisture content changes on remolded strength. Quaternary International, 24: 5−15. DOI：10.1016/1040-6182(94)90032-9.

Derbyshire E. 2001. Geological hazards in loess terrain with particular reference to the loess regions of China. Earth-Science Reviews, 54(1-3): 231−260. DOI：10.1016/S0012-8252(01)00050-2.

Dong Y, Jia J, Zhang MS, et al. 2013. An analysis of the inducing effects of irrigation and the responses of loess landslides in Heifangtai area. Geological Bulletin of China, 32(6): 893−898. (in Chinese) DOI：10.3969/j.issn.1671-2552.2013.06.011.

Hou XK, Sai KV, Li TL. 2018. Water infiltration characteristics in loess associated with irrigation activities and its influence on the slope stability in Heifangtai loess highland, China. Engineering Geology, 234: 27−37. DOI：10.1016/j.enggeo.2017.12.020.

Jia J, Zhu LF, Hu W. 2013. The formation mechanism and disaster mode of loess landslides induced by irrigation in Heifangtai, Gansu Province: A case study of the 13th landslide in Jiaojiayatou. Geological Bulletin of China, 32(12): 1968−1975. (in Chinese) DOI：10.3969/j.issn.1671-2552.2013.12.011.

Jin YL, Dai FC. 2007. Analysis of loess slope stability due to groundwater rise. Journal of Engineering Geology, 15(5): 599−606. (in Chinese) DOI：10.3969/j.issn.1004-9665.2007.05.004.

Lian BQ, Peng JB, Zhan HB, et al. 2020. Formation mechanism analysis of irrigation-induced retrogressive loess landslides. Caneta, 195: 104441. DOI：10.1016/j.catena.2019.104441.

Lu K, Li F, Pan JW, et al. 2021. Using electrical resistivity tomography and surface nuclear magnetic resonance to investigate cultural relic preservation in Leitai, China. Engineering Geology, 285: 106042. DOI：10.1016/j.enggeo.2021.106042.

Ren XH, Xu Q, Zhao KY, et al. 2020. Effect of repeated infiltration on permeability characteristics of remolded loess. Bulletin of Geological Science and Technology, 39(2): 130−138. (in Chinese) DOI：10.19509/j.cnki.dzkq.2020.0214.

Rustadi, Darmawan IGB, Nandi H, et al. 2022. Groundwater exploration using integrated geophysics method in hard rock terrains in Mount Betung Western Bandar Lampung, Indonesia. Journal of Groundwater Science and Engineering, 10(01): 10−18. DOI: 10.19637/j.cnki.2305-7068.2022.01.002.

Song DY, Zhang MS, Mu HD, et al. 2018. Research on the evolution mechanism of deformation and failure of No. 13 landslide in the north of Jiaojiayatou. Geological Bulletin of China, 37(7): 1360−1364. (in Chinese) DOI: 10.12097/j.issn.1671-2552.2018.07.019.

Song HW, Xia F, Mu HD, et al. 2020. Study on detecting spatial distribution availability in mine goafs by ultra-high density electrical method. Journal of Groundwater Science and Engineering, 8(3): 281−286. DOI: 10.19637/j.cnki.2305-7068.2020.03.008.

Tian ZY, Zhang MS, Feng L, et al. 2019. Preferential passage detection of loess landslide based on integrated geophysical exploration. Northwestern Geology, 52(2): 172−180. (in Chinese) DOI: 10.19751/j.cnki.61-1149/p.2019.02.01.

Wang JD, Liu Y. 1999. A further study on the mechanism of high speed loess landslide in state of creeping and sliding lique faction. Journal of Northwest University (Natural Science Edition), 19(001): 79−82. (in Chinese) DOI: 10.1088/0256-307X/16/9/027.

Wang JD, Hui YH. 2001. Systems analysis on Heifangtai loess landslide in crows induced by irrigated water. Bulletin of Soil and Water Conservation, 21(3): 10−13. (in Chinese) DOI: 10.13961/j.cnki.stbctb.2001.03.005.

Wang NQ, Yang PP, Wang DK, et al. 2017. Underground water infiltration area of slope at the edge of loess “yuan”, Heifangtai, Yanguoxia. Journal of Xi’an University of Science and Technology, 37(1): 51−56. (in Chinese) DOI: 10.13800/j.cnki.Xakjdxxb.2017.0109.

Wang ZR, Wu WJ, Zhou ZQ. 2004. Landslide induced by over-irrigation in loess platform areas in Gansu Province. The Chinese Journal of Geological Hazard and Control, 15(3): 43−47. (in Chinese) DOI: 10.16031/j.cnki.issn.1003-8035.2004.03.010.

Wu CX, Xu L, Dai FC, et al. 2011. Topographic features and initiation of earth flows on Heifangtai loess plateau. Rock and Soil Mechanics, 32(6): 1767−1773. (in Chinese) DOI: 10.3969/j.issn.1000-7598.2011.06.028.

Wu WJ, SU X, Feng LT, et al. 2019. The study on landslide types and activity characteristics in Heifangtai, Gansu Province. Journal of Glaciology and Geocryology, 41(6): 1483−1495. (in Chinese) DOI: 10.7522/j.issn.1000-0240.2019.0066.

Xu L, Li HJ, WU DX. 2008. Discussion on infiltration of surface water and their significance to terrace loess landslides. The Chinese Journal of Geological Hazard and Control, 19(2): 32−35. (in Chinese) DOI: 10.3969/j.issn.1003-8035.2008.02.007.

Xu L, Dai FC, Kuang GL, et al. 2009. Characteristics and forming mechanisms of the Plateau-Edge cracks and their significance to loess landslides. Geological Review, 55(1): 85−90. (in Chinese) DOI: 10.16509/j.georeview.2009.01.019.

Xu Q, Peng DL, Qi X, et al. 2016. Dangchuan 2# landsside of April 29, 2015 in Heifangtai area of Gansu Province: Characterisitics and failure mechanism. Journal of Engineering Geology, 24(2): 167−180. (in Chinese) DOI: 10.13544/j.cnki.jeg.2016.02.001.

Xu Q, Qi X, Xiu DH, et al. 2019. Critical water level of abrupt loess landslides: A case study in Heifangtai, Gansu Province. Journal of Hydraulic Engineering, 50(03): 315−322. (in Chinese) DOI: 10.13243/j.cnki.slxb.20190013.

Xu YJ, Gu TF, Wang JD, et al. 2017. An analysis of the influence of the loess fissures flooding effect on slope stability. Hydrogeology & Engineering Geology, 44(4): 154−159. (in Chinese) DOI: 10.16030/j.cnki.issn.1000-3665.2017.04.23.

Ye WL, Kang LJ, An YP, et al. 2021. Analysis of the characteristics and causes of Jiaojia landslide on February 28, 2019 in Yongjing County, Gansu Province. Journal of Lanzhou University (Natural Sciences), 57(3): 369−375. (in Chinese) DOI: 10.13885/j.issn.0455-2059.2021.03.012.

Yu FD, Hao QL, Du H, et al. 2014. Finding out water content characteristic in Heifangtai watering area with geophysical methods. Chinese Journal of Engineering Geophysics, 11(3): 422−425. (in Chinese) DOI: 10.3969/j.issn.1672-7940.2014.03.027.

Zeng L, Jia J. 2022. Instability mechanism and stability trend of loess slope during seasonal Freeze-thaw process. Geological Bulletin of China, 41(8): 1494−1503. (in Chinese) DOI：10.12097/j.issn.1671-2552.2022.08.015.

Zhang FY, Wang GH, Peng JB. 2022. Initiation and mobility of recurring loess flowslides on the Heifangtai irrigated terrace in China: Insights from hydrogeological conditions and liquefaction criteria. Engineering Geology, 302: 106619. DOI：10.1016/j.enggeo.2022.106619.

Zhang Q, Huang GW, Yang CS. 2017. Precision space observation technique for geological hazard monitoring and early warning. Acta Geodaetica et Cartographica Sinica, 46(10): 1300−1307. (in Chinese) DOI：10.11947/j.AGCS.2017.20170453.

Zhang XL, Xu Q, Peng DL, et al. 2017. Application of high-density resistivity method to groundwater exploration in Heifangtai. Progress in Geophysics, 32(4): 1862−1867. (in Chinese) DOI：10.6038/pg20170462.

Zhao JF, Huang JY, Hou XK, et al. 2017. Analysis of a Flow-slide in Heifangtai induced by irrigation. Journal of Catastrophology, 32(4): 60−66. (in Chinese) DOI：10.3969/j.issn.1000-811X.2017.04.010.

Zhao KY, Xu Q, Qi X, et al. 2016. Research on types and characteristics of loess landslides in Gansu Heifangtai. Yangtze River, 47(14): 46−50. (in Chinese) DOI：10.16232/j.cnki.1001-4179.2016.14.011.

Zhou F, Xu Q, Qi X, et al. 2020. The mechanism study of the irrigation-induced sudden loess landslides. Mountain Research, 38(1): 73−82. (in Chinese) DOI：10.16089/j.cnki.1008-2786.000492.

Zhu LF. 2019. Analysis of control factors and external force for the landslides in Heifangtai area. Northwestern Geology, 52(3): 217−222. (in Chinese) DOI：10.19751/j.cnki.61-1149/p.2019.03.020.